

1 **Chemical stabilization of Cd-contaminated soil using fresh and aged wheat straw biochar**

2 Dilani Rathnayake ^{1*}, Filipe Rego ², Reinhart Van Poucke ³, Anthony V. Bridgwater ², Ondřej Mašek ⁴, Erik Meers
3 ³, Jiawei Wang ², Yang Yang ², Frederik Ronsse ¹

4 ¹ Thermochemical Conversion of Biomass Research Group, Department of Green Chemistry and Technology,
5 Faculty of Bioscience Engineering, Ghent University, 653, Coupure Links, 9000, Ghent, Belgium.

6 ² Bioenergy Research Group, EBRI, Aston University, Birmingham, B4 7ET, United Kingdom.

7 ³ Laboratory of Analytical Chemistry and Applied Ecochemistry, Department of Green Chemistry and Technology,
8 Faculty of Bioscience Engineering, Ghent University, 653, Coupure Links, 9000, Ghent, Belgium.

9 ⁴ UK Biochar Research Centre, School of Geosciences, Crew Building, The King's Buildings, University of
10 Edinburgh, Edinburgh, EH9 3FF.

11 *Corresponding author: Dilani Rathnayake (Dilani.RathnayakeMudiyanselage@UGent.be), Thermochemical
12 Conversion of Biomass Research Group, Department of Green Chemistry and Technology, Faculty of Bioscience
13 Engineering, Ghent University, 653, Coupure Links, 9000, Ghent, Belgium.

14 **Highlights**

- 15 • Severity of surface transformation after aging was high in low temperature wheat straw biochar compared
16 to biochar produced at higher temperatures
- 17 • Aged wheat straw biochars performed better than the fresh biochars at 500 °C and 600 °C production
18 temperatures while fresh wheat straw biochar performed better than the aged form only at 400 °C
- 19 • Alkalinity and surface functionality in wheat straw biochar played an important role in immobilization of
20 Cd in pore water

21 **Abstract**

22 Metal mining and smelting activities can introduce a substantial amount of potentially toxic elements (PTE) into
23 the environment that can persist for an extended period. That can limit the productivity of the land and creates
24 dangerous effects on ecosystem services. The effectiveness of wheat straw biochar to immobilize Cd in
25 contaminated soil due to metal smelting activities was investigated in this study. The biochar carbon stability and
26 long-term provisioning of services depend on the biochar production conditions, nature of the feedstock, and the
27 biotic and abiotic environmental conditions in which the biochar is being used. Within this context, three types of

28 wheat straw biochar were produced using a screw reactor at 400 °C, 500 °C, and 600 °C, and tested in a laboratory
29 incubation study. Soil was amended with 2 wt. % of biochar. Both fresh and aged forms of biochar were used.
30 Biochars produced at lower temperatures were characterized by lower pH, a lower amount of stable C, and higher
31 amounts of acidic surface functional groups than the freshly produced biochars at higher production temperatures.
32 At the end of the six months of incubation time, compared to the soil only treatment, fresh and aged forms of wheat
33 straw biochar produced at 600 °C reduced the Cd concentration in soil pore water by 22% and 15% respectively.
34 Our results showed that the aged forms of biochar produced at higher production temperatures (500 °C and 600
35 °C) immobilized Cd more efficiently than the aged forms of lower temperature biochar (400 °C). The findings of
36 this study provide insights to choose the production parameters in wheat straw biochar production while
37 considering their aging effect to achieve successful stabilization of Cd in contaminated soils.

38 **Keywords:** Wheat straw biochar, Accelerated aging, Soil remediation, Biochar stability, Cd contaminated soil

39 1. Introduction

40 Contaminated soil and groundwater can cause adverse impacts on flora and fauna in the surrounding environment.
41 The presence of an elevated amount of potentially toxic elements (PTE) in the soil compared to the natural level
42 is one of the main reasons for soil pollution (Beesley et al., 2011). Soil pollution due to PTEs can happen due to
43 various reasons (e.g. anthropogenic activities such as mining and smelting of metals, mismanagement of hazardous
44 waste, disposal of sewage sludge, waste incineration and chemical waste released from industry or agriculture)
45 (Eugenio et al., 2018; WHO, 2007). The risk and impact posed by PTEs are not solely dependent on the total
46 concentration of a particular PTE in soil. The bioavailable fraction (of a specific PTE) to plants and animals depend
47 on multiple factors, such as soil organic matter content, soil pH, and the soil's cation exchange capacity (Meers et
48 al., 2005). In this context, the remediation of contaminated lands needs to be performed to minimize the harmful
49 impacts on the environment.

50 There are various in-situ and ex-situ methods being used to remediate contaminated soil. Depending on the
51 scenario, a single or a combination of chemical (e.g. oxidation, reduction, pH manipulation), physical (e.g.
52 solidification, washing and treatment) or biological (e.g. phytostabilization, land farming, phytodegradation)
53 remediation methods can be used as a soil remediation process (Ahmad et al., 2014). Sustainable remediation of
54 soil will help to eliminate the risks associated with the contaminants safely, while maximizing the socio-economic
55 and environmental benefits (Beesley et al., 2011; Eugenio et al., 2018). In this context, biochar as an organic soil
56 amendment is becoming popular due to its various advantageous characteristics for contaminated soil remediation
57 (Palansooriya et al., 2020).

58 Biochar is a product of pyrolysis (together with non-condensable pyrolysis gases and bio-oil). Production of
59 biochar is carried out in an oxygen-limited or oxygen-free environment in a temperature range of 350 °C to 700
60 °C (Crombie et al., 2013). Production of biochar provides a more sustainable and economical approach when co-
61 generation and utilization of non-condensable gases and bio-oil is integrated to the system (Lehmann and Joseph,
62 2009). Often, non-condensable pyrolysis gas is used for power generation, fuel production, hydrogen and synthetic
63 gas production. On the other hand, bio-oil can be used to derive bio-based platform chemicals, sustainable fuels
64 and to generate combined heat and power (Masek, 2016). The quantity and physicochemical properties of these
65 pyrolysis products vary with the production conditions (Ronsse et al., 2013).

66 When it comes to biochar, it is characterized by high stability due to a high aromatic carbon content (thus, resistant
67 to biodegradation), a high cation exchange capacity and a high pH. All these physicochemical properties of biochar
68 depend on the feedstock material and pyrolysis production conditions such as production temperature and the
69 residence time at production temperature (Mašek et al., 2013; Zhao et al., 2013). To have a consistent quality of
70 biochar over time, production parameters and feedstock materials should be chosen and monitored correctly
71 (Crombie et al., 2013; Ronsse et al., 2013). Biochars produced from different feedstock materials under different
72 pyrolysis production conditions have been studied for the remediation of PTE contaminated soil all over the world
73 (Ahmad et al., 2014; Lomaglio et al., 2018; Van Poucke et al., 2018). Biochar immobilizes or stabilizes the
74 potentially toxic metals in the soil in various ways, such as through ion exchange, complexation by functional
75 groups, physical adsorption, and precipitation (Bandara et al., 2019). The liming potential of biochar, due to its
76 alkaline pH, has an important effect on PTE mobility in contaminated soils (Qi et al., 2018).

77 To facilitate the efficient remediation of contaminated soil, identification of the mechanisms behind PTE
78 immobilization with different soil amendments is important. Moreover, identification of the optimum pyrolysis
79 production conditions that result in biochar with the desired characteristics (PTE immobilization) is also essential
80 (Wang et al., 2020). Therefore in this study, biochars produced at different pyrolysis production temperatures were
81 assessed as a remediation tool. The long-term provisioning of biochar services mainly depends on its stability
82 (Dharmakeerthi et al., 2015; Liang et al., 2008). As mentioned above, biochar is highly recalcitrant to
83 biodegradation due to the highly aromatic nature of its chemical composition. Long term soil incubation studies
84 with biochar in laboratory scale and field-scale studies provide more realistic information regarding its stability
85 compared to short-term laboratory scale incubation studies (Budai et al., 2013). However, these methods could
86 take a lot of time to draw conclusions regarding the stability of biochar and its potential for remediating PTE
87 contaminated soils. Hence, biochar stability proxies have been developed to assess biochar stability directly or

88 indirectly in a quick way. One such proxy is the “Edinburgh stability tool”, an accelerated aging method of biochar
89 based on its initial total carbon content. The chemical biochar aging procedure in the Edinburgh stability tool can
90 be used as a “proxy for environmental aging of biochar for approximately 100 years under temperate conditions”
91 (Cross and Sohi, 2013). Hydrogen peroxide, which is an inexpensive and strong oxidizer, is used as an oxidation
92 agent in this char aging procedure (Huff and Lee, 2016). A comparison of the carbon content in freshly produced
93 biochar versus aged biochar gives an idea about the stability in long-term soil applications, including soil
94 remediation. Changes of a biochar’s initial characteristics through aging are influenced by the biochar production
95 parameters, the nature of the feedstock material and the type of soil used (Heitkötter and Marschner, 2015). Even
96 though the impacts of fresh biochar on soil properties are well documented, less is known about the long-term
97 behavior of biochar in soil (Dong et al., 2017; He et al., 2019).

98 Aging has a significant impact on the biochar surface functionalities. Due to the aging process, the aliphatic-to-
99 aromatic compound ratios in biochar can change (Rechberger et al., 2017). Besides, the aging of biochar reduces
100 the pH and increases oxygen and hydrogen-containing surface functional groups, increases the surface smoothness
101 and hydrophilic nature of biochar, and increases the cation exchange capacity (Cao et al., 2017; Dong et al., 2017;
102 Mukherjee et al., 2014; Rechberger et al., 2017). Therefore, the experimental results obtained using fresh biochar
103 may not be relevant or accurate for the prediction or assessment of the long-term impacts of biochar (Bakshi et al.,
104 2016). Laboratory aging of biochar can be used to assess the long-term impacts of biochar on soil properties
105 (Lawrinenko et al., 2016). Within this context, both fresh and artificially aged biochars produced under different
106 production conditions and a soil contaminated with Cd due to historic metal smelting activities, were used in this
107 study. The objective of this study is to assess the effectiveness of the fresh and aged wheat straw biochar produced
108 under different pyrolysis temperatures to immobilize Cd in the contaminated soil.

109 **2. Materials and methods**

110 **2.1. Soil characterization**

111 The soil used in this study was sampled from the Campine area (51°12'41"N; 5°14'32"E) which is situated between
112 the northeast of Belgium and the southern part of the Netherlands. The soil samples were collected from the top
113 layer (0-25 cm) and this soil was exposed to atmospheric deposition of PTEs such as Cd and Zn due to local metal
114 smelting activities carried out in the past (Meers et al., 2010). Physicochemical properties of the air dried and
115 sieved soil (<2 mm) used in this study are summarized in Table 1. Soil pH was analyzed in a 1:5 (soil: solution)
116 ratio using a Jenway combined pH and electrical conductivity (EC) meter. Pseudo total elemental concentration in
117 the soil was analyzed after *aqua regia* digestion of which the procedure is described in Van Ranst et al., (1999).

118 Table 1. Characteristics of soil used in this study (mean \pm standard deviation). Weight percentage of sand, silt and
119 clay as reported by Meers et al., (2010).

Parameter	unit	value
Sand	%	88
Silt	%	8
Clay	%	4
pH (1:5)	-	6.9 \pm 0.1
Cd	mg/kg	8 \pm 0.1
Cr	mg/kg	11 \pm 0.2
Cu	mg/kg	20 \pm 0.1
Mn	mg/kg	42 \pm 0.5
Ni	mg/kg	3 \pm 0.1
Pb	mg/kg	190 \pm 0.3
Zn	mg/kg	470 \pm 1.8

120

121 2.2. Biochar production

122 Wheat straw pellets with an average diameter of 0.8 cm and a maximum length of 1.6 cm were provided by
123 Agrodieren Company located near Ghent, Belgium. Neither additives nor binders were used during the production
124 of these pellets. The wheat straw pellets were used in their received form for slow pyrolysis experiments. Pyrolysis
125 experiments were conducted in a bench-scale (300 g/h) screw reactor at Aston University. Biochar samples were
126 produced at 400 °C, 500 °C and 600 °C, and with a solid residence time of 3 minutes at the highest treatment
127 temperature. After production, the biochars were stored in plastic containers. Details about the reactor system and
128 the slow pyrolysis process can be found in previous publications (Yang et al., 2018; Yu et al., 2016).

129 2.3. Accelerated aging of wheat straw biochar samples

130 Biochar samples were subjected to accelerated aging which is equal to the aging of biochar under approx. 100
131 years in temperate soil environment using the method described in Cross and Sohi, (2013). Briefly, finely ground
132 biochar samples were oven-dried at 80 °C for 18 hours to eliminate moisture. Then, biochar samples were analyzed
133 for total C content according to the method described in section 2.4.2. Then, a biochar sample representing 0.1 g
134 of C was weighed into a glass test tube and 0.01 moles of H₂O₂ and 7 mL of distilled water were added into the
135 test tube. After mixing the contents of the tube, samples were heated at 80 °C for 48 hours. After the heating step,

136 the tubes were dried at 105 °C in a conventional oven to evaporate the solution inside. Then, the biochar samples
137 were washed with deionized water three times to remove the residual H₂O₂ in the mixtures. Finally, these
138 artificially aged samples were oven-dried at 105 °C for 24 hours and were subsequently used for soil incubation.
139 Aged biochar samples (A) were named as A400, A500 and A600. Fresh biochars (F) were denoted as F400, F500
140 and F600.

141 **2.4. Biochar characterization**

142 **2.4.1. Proximate analysis**

143 Proximate analysis of biochar was done in triplicate according to the modified version of ASTM D1762-84 method
144 described in Enders et al., (2017). Porcelain crucibles with biochar samples were covered and heated in a
145 conventional drying oven at 105 °C for 18 hours to determine the moisture content by weight difference.
146 Afterwards, covered crucibles with biochar dried at 105 °C were introduced into a muffle furnace heated to 950
147 °C and samples were kept at 950 °C for 10 minutes to determine the volatile matter content in biochar. The ash
148 content was determined by keeping the crucibles (uncovered) containing biochar at 750 °C for 6 hours in the
149 muffle furnace followed by measuring the ash weight. Finally, the fixed carbon content is determined by difference
150 based on volatile matter and ash content:

$$151 \text{ Fixed carbon content (\%, d. b) = (100 - Ash content - Volatile matter content) } \quad (1)$$

152 **2.4.2. Elemental analysis of biochar samples**

153 Biochar samples were analyzed in triplicate for C, H, N, and S by using a Flash 2000 total elemental analyzer
154 (Thermo Scientific, USA). The oxygen content was determined by difference on a dry ash-free basis. 2, 5-bis (5-
155 tert-butyl-benzoxazol-2-yl) thiophene (BBOT) was used as standard reference material during CHNS analysis.

156 **2.4.3. pH and EC of biochar samples**

157 pH and electrical conductivity (EC) of biochar samples were measured in a 1:20 (w/v) ratio with deionized water
158 after shaking for 1 hour and 30 minutes using a Jenway combined pH and EC meter. The analysis was performed
159 in triplicate for each sample.

160 **2.4.4. FTIR analysis of biochar samples**

161 The samples were analyzed qualitatively for surface chemical functionalities using Fourier Transform Infra-Red
162 (FTIR), with a Perkin Elmer Frontier FTIR Spectrometer, with PIKE Technologies GladiATR (Attenuated Total
163 Reflectance) and Spectrum software. The analyses were performed from a wavenumber of 4000 to 400 cm⁻¹, with
164 4 cm⁻¹ resolution using 16 scans.

165 **2.5. Soil incubation experiment and soil pore water extraction**

166 A six-month laboratory soil incubation experiment was conducted to assess the Cd immobilization in contaminated
167 soil with biochar. Four grams of biochar (either fresh or aged) were mixed with 196 g of soil. A control treatment
168 with 200 g of soil was also included. The samples were kept in 0.5 L wide-mouth mason jars covered with parafilm
169 and incubated for six months. The soil moisture content was adjusted to 70 % of the water holding capacity at the
170 beginning of the incubation and maintained over the incubation period. The seven treatment combinations (6
171 amendments and one control soil) were replicated 3 times. Rhizon extractions were done once a month for up to
172 six months to extract the pore water in the treatment mixtures using soil moisture samplers (Eijkelkamp soil
173 moisture samplers, Giesbeek, The Netherlands). After each rhizon extraction, the moisture content of the mixture
174 was readjusted with deionized water by correcting the weight of the jars containing the soil and biochar mixture.

175 **2.6. Sequential extraction**

176 At the end of the six months of incubation, all the treatments were subjected to sequential extraction, according to
177 the method described in (Rauret et al., 1999). Briefly, the exchangeable and weak acid-soluble fraction was
178 extracted using 0.11 M acetic acid (VWR chemicals, Belgium). The reducible fraction (Fe and Mn bound oxides
179 and hydroxides) was extracted using 0.5 M hydroxylamine hydrochloride (Sigma Aldrich, Belgium). The
180 oxidizable fraction (organic matter bound) was extracted using 8.8 M hydrogen peroxide (VWR chemicals,
181 Belgium) and 1 M ammonium acetate (VWR chemicals, Belgium). Then, the residual fraction was determined
182 using the *Aqua regia* soil digestion method (Rauret et al., 1999). Finally, all the extracted samples were analyzed
183 for Cd²⁺ using ICP-OES (Varian Vista-MPX CCD Simultaneous, Varian Inc., Victoria, Australia) and ICP-MS
184 (ELAN DRCE, Perkin Elmer SCIEX, Waltham, MA, USA). Initial soil sample weights were corrected for moisture
185 content and the results are presented on a percentage dry weight basis at 105 °C.

186 **2.7. Statistical analysis**

187 Statistical analyses were performed using IBM's SPSS 22 and Microsoft Excel softwares. The difference in soil
188 pore water pH values, Cd concentrations in different soil fractions, and Cd concentrations in soil pore water
189 between different treatments were assessed using Tukey's post hoc test at a significance level of 0.05. This was
190 done after a one-way ANOVA test. Prior to the ANOVA test, normality was tested using Shapiro-Wilks test for
191 normality and Leven's test.

192

193 **3. Results and discussion**

194 **3.1. Biochar characteristics**

195 The chemical characterization of biochar was performed in order to assess the changes in biochar with pyrolysis
196 production temperature and after accelerated aging. Results are shown in Table 2.

197 Table 2. Characteristics of biochars used in this study (mean \pm standard deviation, n=3).

	Unit	F400	A400	F500	A500	F600	A600
Volatile matter	% (d.b)	35.2 \pm 3.1	49.1 \pm 2.2	30.3 \pm 1.8	43.1 \pm 2.5	19.5 \pm 2.7	34.3 \pm 1.1
Ash	% (d.b)	12.2 \pm 1.2	11.2 \pm 0.1	15.5 \pm 2.1	13.3 \pm 0.5	17.1 \pm 1.3	16.3 \pm 0.8
Fixed carbon	% (d.b)	53.1 \pm 2.1	40.2 \pm 1.1	55.4 \pm 1.6	44.2 \pm 2.4	64.1 \pm 3.2	50.3 \pm 2.5
Total C	% (d.b)	59.3 \pm 2.7	48.1 \pm 1.3	66.2 \pm 3.1	57.5 \pm 0.6	71.2 \pm 1.5	68.1 \pm 2.1
Total H	% (d.b)	0.5 \pm 0.1	0.7 \pm 0.1	0.6 \pm 0.2	1.0 \pm 0.1	0.2 \pm 0.0	0.5 \pm 0.1
Total N	% (d.b)	4.0 \pm 0.2	3.1 \pm 0.5	3.2 \pm 0.2	2.2 \pm 0.3	3.1 \pm 0.1	2.0 \pm 0.1
Total O	% (d.b)	24.5 \pm 1.5	37.3 \pm 2.2	15.4 \pm 1.5	26.8 \pm 0.9	8.8 \pm 0.5	13.5 \pm 1.2
H/C molar ratio	-	0.1 \pm 0.0	0.2 \pm 0.0	0.1 \pm 0.0	0.2 \pm 0.0	0.03 \pm 0.0	0.1 \pm 0.0
O/C molar ratio	-	0.3 \pm 0.0	0.6 \pm 0.0	0.2 \pm 0.0	0.3 \pm 0.0	0.2 \pm 0.0	0.1 \pm 0.0
pH (1:10)	-	9.6 \pm 0.2	5.1 \pm 0.1	9.9 \pm 1.5	6.9 \pm 1.1	10.3 \pm 0.5	8.6 \pm 1.3
EC (1:10)	mS/cm	1.4 \pm 0.1	1.8 \pm 0.4	2.2 \pm 0.1	4.7 \pm 0.3	3.4 \pm 0.1	3.6 \pm 0.2

198

199 **3.1.1. pH and EC**

200 The pH and EC of biochar provide an indication of the alkalinity and salt concentration in biochar. It is well
201 known that in general, with an increase in pyrolysis temperature, acidic functional groups on the surface of biochar
202 (i.e., hydroxyl and carboxyl groups) are progressively being removed. At the same time, because of the
203 volatilization of organic matter, the ash content increases at higher pyrolysis temperatures (Crombie et al., 2013;
204 Nachenius et al., 2013). As a result, the remaining solid product becomes more alkaline (Weber and Quicker,
205 2018) and the biochar pH and EC increase. In this study, the biochar pH varied between 5.1 in A400 to 10.3 in
206 F600. As expected, the biochar pH increased with an increase in pyrolysis temperature and decreased after aging.
207 Huff and Lee, (2016) and Mia et al., (2017) reported that during the aging of biochar by using an oxidizing agent,
208 surface functionalities like carboxylic, phenolic and ether groups can be created. These functional groups are acidic
209 in nature and could introduce acidity into biochar.

210 Depending on the aromaticity of biochar, the nature and quantity of the surface groups could vary. Lawrinenko et
211 al., (2016) also reported that high-temperature biochar was more resistant to oxidation and to loss of anion
212 exchange capacity than biochar produced at lower production temperatures. This is more likely the reason for the
213 drastic pH reduction in A400 compared to F400. As a result of the formation of oxygenated functionalities on the
214 surface of biochar induced by aging, the negative charge on the surface could increase. Carboxylate groups formed
215 during oxidation can convert into carboxyl groups (Lawrinenko et al., 2016). A400 and A500 samples had slightly
216 acidic pH and all the other biochar samples had highly alkaline pH values. Only the A400 sample had a pH lower
217 than the soil pH value (Table 2). The electrical conductivity of the biochar samples ranged between 1.4 mS/cm in
218 A400 to 3.6 mS/cm in A600. The EC of biochar increased with the pyrolysis production temperature and with the
219 aging of biochar.

220 **3.1.2. Proximate composition**

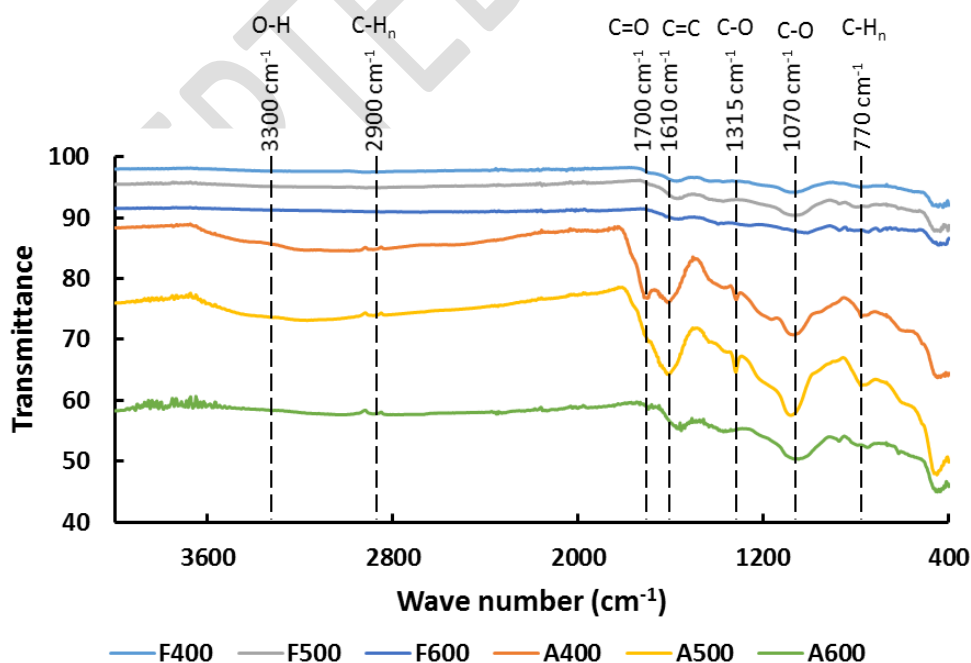
221 The fixed carbon content of wheat straw biochar increased with an increase in pyrolysis production temperature.
222 However, its value decreased after the aging procedure. In fresh biochar samples, fixed carbon content varied
223 between 53% (d.b) in F400 to 64% (d.b) in F600. In aged biochar samples, fixed carbon content varied between
224 40% (d.b) in A400 and 50% (d.b) in A600 (Table 2). At higher pyrolysis production temperatures, the ash content
225 in biochar samples was higher and the volatile matter content was lower. The highest ash content was in F600
226 (17%, d.b.) and the lowest ash content was in A400 (11%, d.b.). Volatile matter content was lowest for F600 (19%,
227 d.b), while the highest was observed for A400 (49%, d.b). From these observations, it is clear that non-volatile ash
228 accumulates in the biochar as the pyrolysis temperature increases while simultaneously, volatile matter is
229 progressively removed. With accelerated aging, the ash content in biochar lowered and volatile matter content
230 increased. However, the reduction in ash content after aging was not significant. During the aging with an oxidizing
231 agent (which was in the form of an aqueous solution), removal of labile carbon and accessible salts could happen
232 (Mia et al., 2017). Some salts and minerals attached to the biochar structure could become more labile and partial
233 oxidation of fixed carbon to more labile forms could happen during the aging process (Mia et al., 2017). As a
234 result, a decrease in fixed carbon content and ash content, together with an increase in volatile matter content
235 occurs (Bakshi et al., 2016). This observation aligns well with the increase in pH and EC of biochar with pyrolysis
236 production temperature and the decrease of pH and EC upon char aging.

237 **3.1.3. Elemental analysis**

238 The total C content in biochar samples ranged from 48% (d.b) in A400 to 71% (d.b) in F600 (Table 2). With the
239 increase in pyrolysis production temperature, biochar total C content increased, and as a result, the H/C molar ratio

240 decreased. As the H/C molar ratio is a proxy for biochar stability, it can be concluded that the stability of the
 241 biochar samples increased at higher production temperature (Budai et al., 2013). The total N content decreased
 242 with the pyrolysis temperature and after accelerated aging of biochar samples. This may be due to a loss of protein
 243 associated chemical functionalities (like amines and amides) in the feedstock with an increase in pyrolysis
 244 temperature. Due to the degradation of cellulose, hemicellulose, and lignin during pyrolysis, a release of volatiles
 245 occurs (Ronsse et al., 2015). As a result, the produced biochars had a more condensed aromatic structure with
 246 higher aromatic carbon content than the feedstock material. Elimination of H and N embedded in weaker (i.e.
 247 thermally labile) functional groups with an increase in pyrolysis temperature results in biochar with lower H and
 248 N contents (Crombie et al., 2013). With the increase in pyrolysis production temperature, C content in biochar and
 249 the degree of aromatization increase. As a result of that, oxygen functionalities on the biochar surface decrease
 250 (Chen et al., 2016). During the aging process, degradation of pyrrole and pyridine structures could happen. This
 251 may contribute to the observed reduction of N in aged biochar (Lawrinenko et al., 2016). Also, due to the H
 252 attachments by radical formation to the basal planes of condensed aromatic carbons, the total H content in aged
 253 biochar increases (de la Rosa et al., 2018). As aging progresses, surface functional groups containing oxygen are
 254 formed. As a result, total oxygen content in aged biochar increased (Lawrinenko et al., 2016) (Table 2).

255 3.1.4. FT-IR analysis of biochar



256

257 **Fig. 1** FTIR spectra for the fresh (F) and aged (A) biochars produced from slow pyrolysis of wheat straw at 400,

258 500 and 600 °C.

259 The fresh and aged biochars from wheat straw were analyzed using FTIR to qualitatively determine surface
260 chemical functionalities. The spectra are displayed in Fig 1. During the accelerated aging process of biochar,
261 oxygen-containing surface functional groups are formed. Those functional groups can be acidic, neutral or alkaline
262 in nature (Huff and Lee, 2016; Lawrinenko et al., 2016). Acidic functionalities that are created after aging, such
263 as carboxylic, hydroxyl, quinone, phenolic, lactonic groups could make biochar more hydrophilic, with higher
264 surface area and porosity (Beesley et al., 2011; Cheng et al., 2008). The aging-induced oxygen-containing
265 functional groups may be responsible for lowering the biochar pH after aging (Table 2). However, the quantity
266 and the nature of functional groups is based on the intensity of the aging treatment and the chemical agent used
267 (Moreno-Castilla et al., 1995). According to that, aging with H₂O₂ produces more carbonyl and carboxylate
268 functionalities (Beesley et al., 2011; Cheng et al., 2008). The increase in oxygen proportion by using H₂O₂ can be
269 confirmed with elemental analysis (Table 2). Singh et al., (2014) also observed through XPS analysis, that biochar
270 gained more carboxyl groups on its surface after aging. In the region of O-H bond vibration at around 3300 cm⁻¹,
271 a band can be seen for the aged biochars, especially the ones produced at 400 °C and 500 °C. This indicates an
272 increase in the presence of alcohols and phenols. A lack of peaks in the region 2850-2950 cm⁻¹, corresponding to
273 the stretching vibration of C-H_n bonds, both for the fresh and aged biochars, indicates that aliphatic compounds
274 had a relatively low presence in fresh biochars and that they were not produced by oxidation using H₂O₂. The
275 intensity of aging of biochar (i.e. increase in O-containing surface functional groups) after treating with H₂O₂ is
276 affected by the pyrolysis production conditions during biochar production and similar observations were reported
277 by Cheng et al., (2008).

278 For wavenumbers around 1700-1800 cm⁻¹, which correspond to C=O bonds (carbonyls), some bands can be seen
279 for the aged biochar produced at 400 °C pyrolysis temperature. There is also some bands in the aged 500 °C
280 biochar, but not for the 600 °C aged biochar. This relates to the fact that the surface of the biochars produced at
281 lower pyrolysis temperatures is more prone to chemical transformation by oxidation because more surface
282 functionalities are present, thus enabling the creation of more O-containing compounds on the surface than the
283 biochars obtained at higher pyrolysis temperatures. In the region of the spectrum between 1550 and 1650 cm⁻¹,
284 which corresponds to vibrating C=C bonds (e.g. aromatics), there is a significant manifestation for the aged
285 biochars from 400 °C and 500 °C pyrolysis, but not as significant for the 600 °C aged biochar or the fresh biochars.
286 The presence of alcohols and carboxylic acids, and also esters and ethers, is indicated by the strong band located
287 at 1000-1150 cm⁻¹ and other peaks (e.g. around 1320 cm⁻¹) at 1100-1320 cm⁻¹ (vibration of C-O bonds). These
288 regions have IR manifestations in the spectra for the aged biochars, and much less for the freshly-produced

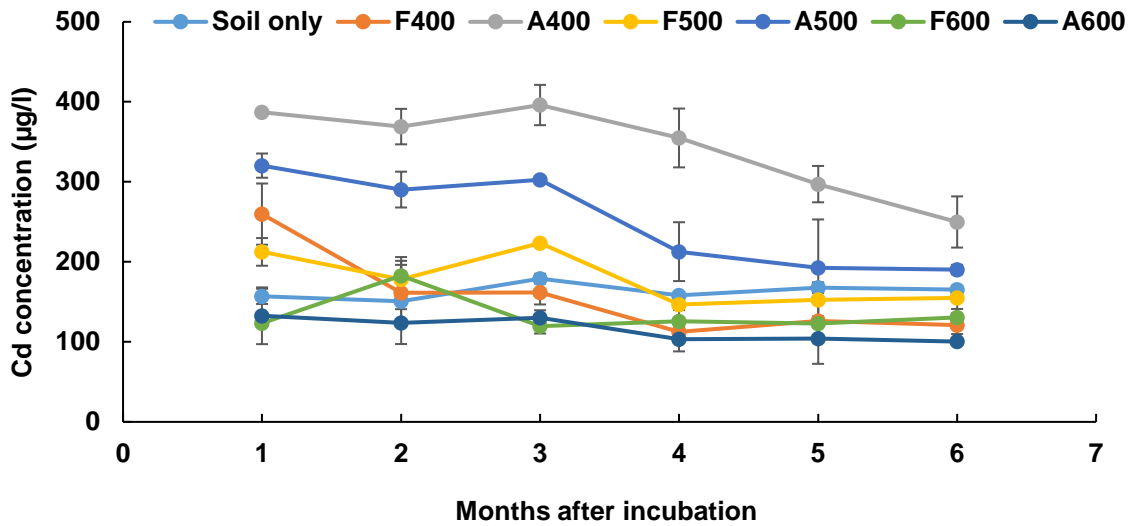
289 biochars. This is corroborated by the elemental analysis in Table 2, which shows increases of O content for the
290 aged biochars. The formation of carboxylate groups on the surface increases negative surface charge and CEC but
291 does not change anion exchange capacity (Lawrinenko et al., 2016; Oustriere et al., 2017).

292 It can be concluded from the FTIR analysis that the aging process has significantly changed the surface chemistry
293 of the wheat straw biochars, and more significantly the ones produced at 400 °C and 500 °C, compared to the one
294 from 600 °C. This result is related to the temperature of the pyrolysis process (i.e. the higher the applied
295 temperature is the more the surface functionalities are reduced, and the more stable the produced biochar is). This
296 temperature effect leaves more functionalities available for oxidation with H₂O₂ on the biochars from lower
297 pyrolysis temperatures. The changes on the surface were mainly translated into increases in functional groups such
298 as carboxyl and hydroxyl groups. The increase in surface functional groups with H₂O₂ oxidation, e.g. polar groups,
299 can potentially lead to better performance in applications such as liquid-phase adsorption and soil amendment,
300 with increased retention of nutrients for plant growth and lower mobility of PTE such as Zn (Bashir et al., 2018;
301 Kumar et al., 2018). For example, the retention of PTE ions such as Cd (II) was found to be favored by the presence
302 of O-containing functional groups that act as binding sites, such as –OH and –COOH, e.g. through complexation
303 (Sun et al., 2014; Zuo et al., 2016).

304 3.2. Changes in soil pore water Cd concentration and pH

305 The Cd concentration in rhizon soil pore water extracts over a 6 months of period is depicted in
306 **Fig. 2.** When the soil was mixed with biochar, in the initial soil and biochar mixtures, the pH had values of $8.1 \pm$
307 0.3 (F400), 5.2 ± 0.1 (A400), 8.8 ± 0.1 (F500), 6.3 ± 0.1 (A500), 9.1 ± 0.2 (F600) and 7.5 ± 0.2 (A600). Rhizon
308 soil moisture samplers can be used to sample the dissolved components in soil solution. The Cd concentration in
309 the soil pore water is mainly governed by pH, CEC and the total Cd concentration in soil (Meers et al., 2007). At
310 the end of the first month of the incubation, both fresh and aged biochar produced at 400 °C (260 µg/L and 387
311 µg/L in F400 and A400 respectively) and 500 °C (212 µg/L and 320 µg/L in F500 and A500 respectively) had
312 higher Cd concentrations than the soil only (157 µg/L) treatment. Only fresh and aged biochars produced at 600
313 °C had lower Cd concentrations in pore water compared to the control (123 µg/L and 133 µg/L in F600 and A600
314 respectively).

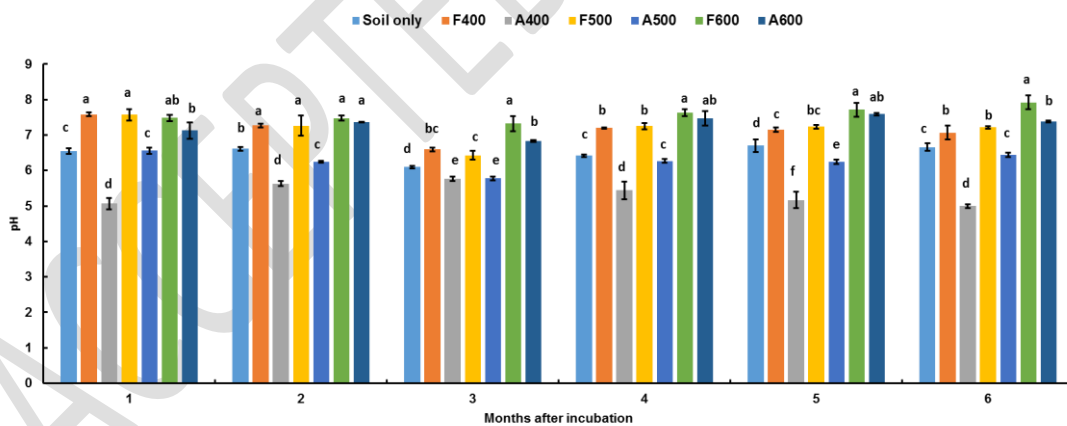
315



316
317
318
319
320
321
322

Fig. 2 Cd concentration in rhizon extracts ($\mu\text{g/L}$) (mean \pm sd, n=3) during a six month incubation experiment.

At the end of the six month of incubation period, A400 showed a significantly higher level of Cd concentration in the soil solution than the other treatments. Except the A400 treatment, there were no significance differences between the other treatments. This observation is supported by the data and trends of soil solution pH shown in Fig 3.



323
324
325
326
327
328
329

Fig. 3 pH in rhizon extracts (mean \pm sd, n=3) during a six month incubation experiment. Same letters indicate no significant difference at $p < 0.05$ level.

At the beginning of the incubation, A600 and F600 showed a higher pH compared to the other treatments. Also, at the end of the 6 months of incubation, Cd concentration in the soil solution was well aligned with the pH of the soil solution. Previous studies (Xu et al., 2018; Yang et al., 2016) reported that alkalisation is the dominant process in Cd immobilization, which controls the release of Cd into the soil solution. Heavy metal immobilization

330 capacity of biochar depends on several factors, such as the physicochemical characteristics of biochar, the
331 application dose of biochar in soil, the Cd concentration in the soil and the physicochemical properties of the soil
332 such as pH, redox potential, organic matter content, moisture content and the nature of the mineral constituents
333 (Bandara et al., 2019; Xu et al., 2013). Based on the above findings, except for the A400 biochar treatment, all
334 aged biochar treatments (A500 and A600) efficiently immobilized the Cd in both the exchangeable fraction and
335 the rhizon pore water extracts. According to past studies (Reverchon et al., 2015; Tan et al., 2015; Zhao et al.,
336 2020), there are few underlying mechanisms that can be identified as responsible for Cd immobilization in soil.
337 These include the formation of insoluble compounds (precipitates) via reactions between Cd^{2+} ions and biochar
338 mineral constituents (i.e., carbonates and phosphates), physical adsorption of Cd^{2+} in soil pores and/or in biochar
339 pores through transformed metal species via redox reactions, formation of surface complexation between Cd^{2+} and
340 functional groups on biochar surface (i.e., hydroxide and carboxylic groups), electrostatic interaction between
341 biochar and Cd^{2+} , and ion exchange via Cd^{2+} and protons and alkaline metals in biochar.

342 Increase in pH through the addition of lime or limestone decreases the metal solubility through sorption and the
343 formation of less soluble precipitates (Ettler, 2016; Liang et al., 2014). Therefore, having a constant pH in soil and
344 soil pore water is crucial in remediation processes (Van Poucke et al., 2020; Zheng et al., 2017). Moreover, Qi et
345 al., (2018) observed a higher solubility of Cd under acidic conditions. Reduction in Cd mobility in soil pore water
346 under acidic conditions could be due to a reduction in surface complexation of Cd^{2+} onto biochar surface
347 functionalities (Qi et al., 2018). The increase in soil pH reduces the bioavailable Cd due to an increase in surface
348 negative charges and therefore an increase in negative charge densities and exchange sites. This is well backed up
349 by the decrease in Cd in pore water when biochar pH increases (Fig A.1. in appendix). The presence of highly
350 dissolved organic carbon (DOC) could increase the metal mobility through an increase of soluble organometallic
351 complexes which could decrease the adsorption of metals (Egene et al., 2018). Dong et al., (2017) observed that
352 aged biochar consisted of smooth surfaces, larger pores and newly formed small pores. Due to this, even with the
353 reduced pH in aged biochar added treatments, it was possible to reduce the pore water Cd concentration due to an
354 increase in sorption sites (Fig 2).

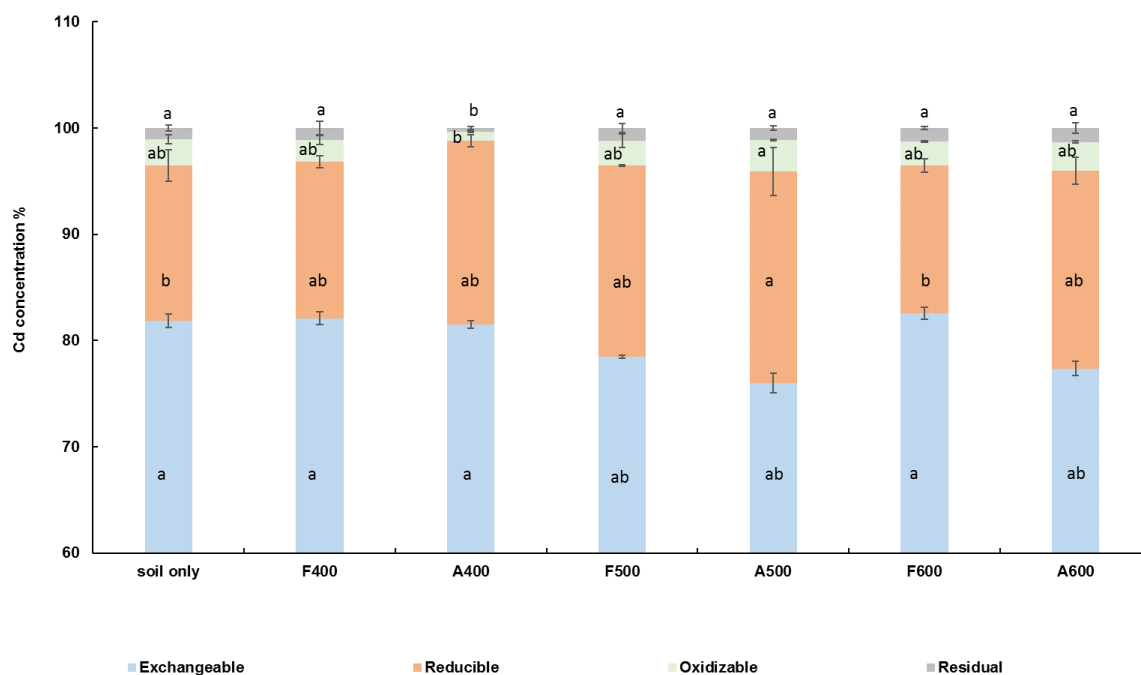
355 Oxidation of biochar could introduce additional binding sites for Cd^{2+} through an increase in functional groups on
356 the biochar surface. As mentioned in section 3.1.4., the strong bands related to carbonyl and carboxyl
357 functionalities on aged low temperature biochar (A500 and A400) are likely to contribute to binding of Cd^{2+} and
358 reduce their availability in the pore water (Tan et al., 2015). A500 and A600 performed well even though those
359 biochars have acidic pH compared to A400. Therefore, availability of Cd in pore water is governed by the

360 combined effect of pH and surface complexation via functional groups on the surface of biochar. In this study it
361 appears that the effectiveness of this process is mainly governed by soil pore water pH (Appendix, Fig A.1.).

362 3.3. Sequential extraction

363 The distribution of the different fractions of Cd in the soil among the different treatments are presented in Fig 4.

364 The Cd concentration in different geochemical soil fractions gives an idea about its mobility in the soil. The
365 exchangeable fraction contains the PTEs that affect the sorption and desorption processes. PTEs that are bound to
366 Fe and Mn oxides and unstable under anoxic conditions represent the reducible fraction.



367
368 **Fig. 4** Distribution (in %) of different fractions of Cd in soil among different treatments (mean± sd, n=3). Same
369 letters indicate no significant difference at p<0.05 level

370 The organic matter-bound fraction contains the PTEs bound to organic matter derived from plant and animal
371 detritus materials (Rauret et al., 1999; Tessier et al., 1979). Those PTEs could be released to the soil solution due
372 to the degradation of organic matter by oxidation. The residual fraction, which is mostly the unavailable fraction
373 contains the PTEs trapped into primary and secondary mineral structures (Tessier et al., 1979).

374 In the exchangeable fraction, only F500, A500, and A600 had a significantly lower concentration of Cd than the
375 other treatments (F400, A400 and F600) and the control. The exchangeable fraction in soil mainly depends on the
376 soil pH and the availability of binding sites. The alkalinity of biochar is beneficial to Cd binding. However, this
377 could be less effective with an increase in soil acidification or upon aging of biochar (Qian et al., 2015; Xu et al.,

378 2016). On the other hand, aging of biochar could increase the biochar's H/C molar ratio, O/C molar ratio, specific
379 surface area and porosity (Hardy et al., 2017). Aged biochars could have more acidic functionalities (Fig 1) and
380 be more hydrophilic (Lian and Xing, 2017). Thus, aged biochars can attract more positively charged cations like
381 Cd^{2+} through electrostatic attraction and surface complexation. This is well supported by the lower Cd
382 concentrations in the exchangeable fraction in A500 and A600 (**Fig. 4**).

383 As mentioned in section 3.2, at the end of the six month incubation period, soil pore water Cd was significantly
384 higher only in A400 compared to the other treatments including soil only. The difference in the observation
385 between the pore water Cd and CaCl_2 -extractable Cd may be due to a difference in the extraction methods. Both
386 pore water extraction by rhizon soil moisture sampling and CaCl_2 extraction occur under actual soil pH without
387 buffering. However, compared to rhizon extraction, CaCl_2 extraction is accompanied by strong divalent cation
388 exchange. Also, chloride as a counter ion could cause additional complexation and mobilization of PTEs (Meers
389 et al., 2007). On the other hand, F400 and F600 had a lower amount of surface functionalities (i.e., carboxylic,
390 carbonate and carbonyl functionalities) compared to A400 and A600. Consequently, the fresh biochars retain more
391 Cd^{2+} ions into the exchangeable fraction even under favorable pH conditions (**Fig. 4**).

392 Only the A500 treatment had significantly higher levels of Cd in the reducible fraction than the other treatments.
393 Reduction of Cd concentration in the exchangeable fraction in A500 can be connected to the increase in the Cd
394 concentration in the reducible fraction. Besides A400, all the other treatments had significantly higher Cd
395 concentrations in organic matter bound fraction. There was not any significant difference observed between soil
396 only, F500, F600 and A600 treatments in organic matter bound fraction (**Fig. 4**). Organic matter can bind
397 contaminants (i.e. cations) through its negatively charged sites (Ettler, 2016). Aging of biochar could increase its
398 organic matter bound fraction due to an increase in negative charges on the biochar surface (Egene et al., 2018).
399 This fits well with the significantly higher Cd concentrations in the organic matter bound fraction in aged biochar
400 treatments (A500 and A600) than the fresh biochar treatments (**Fig. 4**). Moreover, having higher amount of acidic
401 functionalities in aged biochar compared to fresh forms are favorable to surface complexation of Cd with organic
402 matter (**Fig. 1**). Compared to soil only treatment, only A400 had significantly lower Cd concentration in the
403 residual fraction. This may be due to an interruption of the Cd precipitation mechanisms due to higher acidity in
404 the A400 treatment compared to the other treatments.

405 **4. Conclusions**

406 The effect of aging on biochar's ability to immobilize Cd was tested using wheat straw biochar produced at
407 different temperatures. Alkalinity and surface complexation via functional groups were identified as the primary
408 mechanisms contributing to the Cd immobilization. Therefore, the changes with aging to these properties have
409 been the key driver behind the differences in Cd immobilization between fresh and aged biochar. Aging has
410 resulted in biochar with less alkaline pH and more acidic surface functionalities compared to fresh biochars. The
411 severity of this effect was higher in biochar produced at a lower temperature compared to biochar produced at
412 higher production temperatures. Both A500 and A600 effectively immobilized the Cd in pore water compared to
413 A400. Hence, biochar produced at lower temperature is more effective in the short term, while biochar produced
414 at higher production temperature is more beneficial for longer-term stabilizing effects. Thus, wheat straw biochar
415 produced at higher production temperatures (i.e., 500 °C and 600 °C) is more beneficial for long-term stabilizing
416 of Cd in contaminated Lommel soil due to the favorable combined effect of pH and surface functionalities. The
417 findings of this study provide insights to choose the production parameters in wheat straw biochar production
418 while considering their aging effect to achieve a successful stabilization of Cd in contaminated soils.

419 **Declaration**

420 Ethics approval and consent to participate – Not applicable

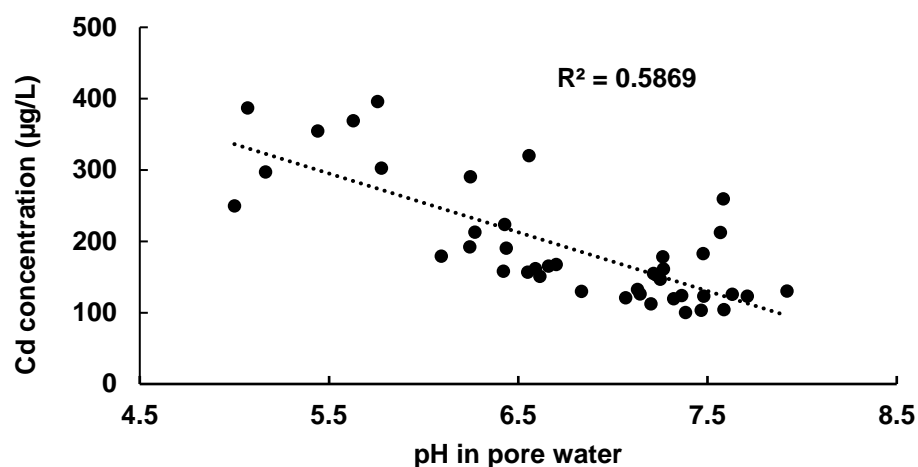
421 Consent for publication – Not applicable

422 Availability of data and materials –All data generated or analysed during this study are included in this article.

423 Competing interests – The authors declare that they have no competing interests

424 Funding - Results incorporated in this paper received funding from the European Union's Horizon 2020 research
425 and innovation programme under the Marie Skłodowska-Curie grant agreement No 721991.

426 Author contributions - **DR**: Conceptualization, investigation, formal analysis, visualization, writing original draft,
427 **FR**: Investigation, writing-review and editing, **RVP**: Investigation, writing-review and editing, **AVB, OM, EM,**
428 **JW**, and **YY**: Supervision, resources, writing-review and editing, **FR**: Supervision, resources, writing-review and
429 editing and funding acquisition. All authors read and approved the final manuscript.



431

432 **Fig A.1** Relationship between pore water pH and Cd concentration.433 **References**

- 434 Ahmad, M., Rajapaksha, A.U., Lim, J.E., Zhang, M., Bolan, N., Mohan, D., Vithanage, M., Lee, S.S., Ok, Y.S.,
 435 2014. Biochar as a sorbent for contaminant management in soil and water: a review. *Chemosphere* 99, 19–
 436 33. <https://doi.org/10.1016/j.chemosphere.2013.10.071>
- 437 Bakshi, S., Aller, D.M., Laird, D.A., Chintala, R., 2016. Comparison of the Physical and Chemical Properties of
 438 Laboratory and Field-Aged Biochars. *J. Environ. Qual.* 45, 1627. <https://doi.org/10.2134/jeq2016.02.0062>
- 439 Bandara, T., Franks, A., Xu, J., Bolan, N., Wang, H., Tang, C., 2019. Technology Chemical and biological
 440 immobilization mechanisms of potentially toxic elements in biochar-amended soils. *Crit. Rev. Environ. Sci.*
 441 *Technol.* 3389. <https://doi.org/10.1080/10643389.2019.1642832>
- 442 Bashir, S., Zhu, J., Fu, Q., Hu, H., 2018. Comparing the adsorption mechanism of Cd by rice straw pristine and
 443 KOH-modified biochar. *Environ. Sci. Pollut. Res.* 25, 11875–11883. <https://doi.org/10.1007/s11356-018-1292-z>
- 445 Beesley, L., Moreno-Jiménez, E., Gomez-Eyles, J.L., Harris, E., Robinson, B., Sizmur, T., 2011. A review of
 446 biochars' potential role in the remediation, revegetation and restoration of contaminated soils. *Environ.*
 447 *Pollut.* 159, 3269–3282. <https://doi.org/10.1016/j.envpol.2011.07.023>
- 448 Budai, A., Zimmerman, A.R., Cowie, A.L., Webber, J.B.W., Singh, B.P., Glaser, B., Masiello, C.A., 2013. Biochar

449 Carbon Stability Test Method : An assessment of methods to determine biochar carbon stability.

450 Cao, T., Chen, W., Yang, T., He, T., Liu, Z., Meng, J., 2017. Surface characterization of aged biochar incubated
451 in different types of soil. *BioResources* 12, 6366–6377. <https://doi.org/10.15376/biores.12.3.6366-6377>

452 Chen, D., Yu, X., Song, C., Pang, X., Huang, J., Li, Y., 2016. Effect of pyrolysis temperature on the chemical
453 oxidation stability of bamboo biochar. *Bioresour. Technol.* 218, 1303–1306.
454 <https://doi.org/10.1016/j.biortech.2016.07.112>

455 Cheng, C.H., Lehmann, J., Thies, J.E., Burton, S.D., 2008. Stability of black carbon in soils across a climatic
456 gradient. *J. Geophys. Res. Biogeosciences* 113, 1–10. <https://doi.org/10.1029/2007JG000642>

457 Crombie, K., Mašek, O., Sohi, S.P., Brownsort, P., Cross, A., 2013. The effect of pyrolysis conditions on biochar
458 stability as determined by three methods. *GCB Bioenergy* 5, 122–131. <https://doi.org/10.1111/gcbb.12030>

459 Cross, A., Sohi, S.P., 2013. A method for screening the relative long-term stability of biochar. *GCB Bioenergy* 5,
460 215–220. <https://doi.org/10.1111/gcbb.12035>

461 de la Rosa, J.M., Rosado, M., Paneque, M., Miller, A.Z., Knicker, H., 2018. Effects of aging under field conditions
462 on biochar structure and composition: Implications for biochar stability in soils. *Sci. Total Environ.* 613–
463 614, 969–976. <https://doi.org/10.1016/j.scitotenv.2017.09.124>

464 Dharmakeerthi, R.S., Hanley, K., Whitman, T., Woolf, D., Lehmann, J., 2015. Organic carbon dynamics in soils
465 with pyrogenic organic matter that received plant residue additions over seven years. *Soil Biol. Biochem.*
466 88, 268–274. <https://doi.org/10.1016/J.SOILBIO.2015.06.003>

467 Dong, X., Li, G., Lin, Q., Zhao, X., 2017. Quantity and quality changes of biochar aged for 5 years in soil under
468 field conditions. *Catena* 159, 136–143. <https://doi.org/10.1016/j.catena.2017.08.008>

469 Egene, C.E., Poucke, R. Van, Ok, Y.S., Meers, E., Tack, F.M.G., 2018. Impact of organic amendments (biochar
470 , compost and peat) on Cd and Zn mobility and solubility in contaminated soil of the Campine region after
471 three years. *Sci. Total Environ.* 626, 195–202. <https://doi.org/10.1016/j.scitotenv.2018.01.054>

472 Enders, A., Sohi, S., Lehmann, J., Balwant, S., 2017. Total elemental analysis of metals and nutrients in biochar,
473 in: *Biochar: A Guide to Analytical Methods*. Csiro Publishing, pp. 95–108.

474 Ettler, V., 2016. Soil contamination near non-ferrous metal smelters : A review. *Appl. Geochemistry* J. 64, 56–74.
475 <https://doi.org/10.1016/j.apgeochem.2015.09.020>

476 Eugenio, N.R., McLaughlin, M., Pennock, D., 2018. SOILPOLLUTION: A HIDDEN REALITY. Food and
477 Agriculture Organization of the United Nations (FAO).

478 Hardy, B., Leifeld, J., Knicker, H., Dufey, J.E., Deforce, K., Cornélis, J., 2017. Long term change in chemical
479 properties of preindustrial charcoal particles aged in forest and agricultural temperate soil. *Org. Geochem.*
480 107, 33–45. <https://doi.org/10.1016/j.orggeochem.2017.02.008>

481 He, E., Yang, Y., Xu, Z., Qiu, H., Yang, F., Peijnenburg, W.J.G.M., Zhang, W., Qiu, R., Wang, S., 2019. Two
482 years of aging influences the distribution and lability of metal(loid)s in a contaminated soil amended with
483 different biochars. *Sci. Total Environ.* 673, 245–253. <https://doi.org/10.1016/j.scitotenv.2019.04.037>

484 Heitkötter, J., Marschner, B., 2015. Interactive effects of biochar ageing in soils related to feedstock , pyrolysis
485 temperature , and historic charcoal production ☆. *Geoderma* 245–246, 56–64.
486 <https://doi.org/10.1016/j.geoderma.2015.01.012>

487 Huff, M.D., Lee, J.W., 2016. Biochar-surface oxygenation with hydrogen peroxide. *J. Environ. Manage.* 165, 17–
488 21. <https://doi.org/10.1016/j.jenvman.2015.08.046>

489 Kumar, A., Joseph, S., Tsechansky, L., Privat, K., Schreiter, I.J., Schüth, C., Graber, E.R., 2018. Biochar aging in
490 contaminated soil promotes Zn immobilization due to changes in biochar surface structural and chemical
491 properties. *Sci. Total Environ.* 626, 953–961. <https://doi.org/10.1016/j.scitotenv.2018.01.157>

492 Lawrinenko, M., Laird, D.A., Johnson, R.L., Jing, D., 2016. Accelerated aging of biochars: Impact on anion
493 exchange capacity. *Carbon N. Y.* 103, 217–227. <https://doi.org/10.1016/j.carbon.2016.02.096>

494 Lehmann, J., Joseph, S., 2009. A Future for Biochar in Vermont. *Biochar Environ. Manag. Sci. Technol.* 416.

495 Lian, F., Xing, B., 2017. Black Carbon (Biochar) In Water / Soil Environments : Molecular Structure , Sorption
496 , Stability , and Potential Risk. *Environ. Sci. Technol.* <https://doi.org/10.1021/acs.est.7b02528>

497 Liang, B., Lehmann, J., Solomon, D., Sohi, S., Thies, J.E., Skjemstad, J.O., Luizão, F.J., Engelhard, M.H., Neves,
498 E.G., Wirick, S., 2008. Stability of biomass-derived black carbon in soils. *Geochim. Cosmochim. Acta* 72,
499 6069–6078. <https://doi.org/10.1016/j.gca.2008.09.028>

500 Liang, Y., Cao, X., Zhao, L., Arellano, E., 2014. Biochar- and phosphate-induced immobilization of heavy metals
501 in contaminated soil and water: Implication on simultaneous remediation of contaminated soil and
502 groundwater. *Environ. Sci. Pollut. Res.* 21, 4665–4674. <https://doi.org/10.1007/s11356-013-2423-1>

503 Lomaglio, T., Hattab-Hambli, N., Miard, F., Lebrun, M., Nandillon, R., Trupiano, D., Scippa, G.S., Gauthier, A.,
504 Motelica-Heino, M., Bourgerie, S., Morabito, D., 2018. Cd, Pb, and Zn mobility and (bio)availability in
505 contaminated soils from a former smelting site amended with biochar. *Environ. Sci. Pollut. Res.* 25, 25744–
506 25756. <https://doi.org/10.1007/s11356-017-9521-4>

507 Masek, O., 2016. Biochar in thermal and thermochemical biorefineries—production of biochar as a coproduct.,
508 in: *Handbook of Biofuels Production*. Woodhead Publishing.

509 Mašek, O., Brownsort, P., Cross, A., Sohi, S., 2013. Influence of production conditions on the yield and
510 environmental stability of biochar, in: *Fuel*. pp. 151–155. <https://doi.org/10.1016/j.fuel.2011.08.044>

511 Meers, E., Du Laing, G., Unamuno, V., Ruttens, A., Vangronsveld, J., Tack, F.M.G., Verloo, M.G., 2007.
512 Comparison of cadmium extractability from soils by commonly used single extraction protocols. *Geoderma*
513 141, 247–259. <https://doi.org/10.1016/j.geoderma.2007.06.002>

514 Meers, E., Slycken, S. Van, Adriaensen, K., Ruttens, A., Vangronsveld, J., Laing, G. Du, Witters, N., Thewys, T.,
515 Tack, F.M.G., 2010. The use of bio-energy crops (*Zea mays*) for ‘ phytoattenuation ’ of heavy metals on
516 moderately contaminated soils : A field experiment. *Chemosphere* 78, 35–41.
517 <https://doi.org/10.1016/j.chemosphere.2009.08.015>

518 Meers, E., Unamuno, V., Vandeghechuchte, M., Vanbroekhoven, K., Geebelen, W., Samson, R., Vangronsveld, J.,
519 Diels, L., Ruttens, A., Du Laing, G., Tack, F., 2005. Soil-solution speciation of Cd as affected by soil
520 characteristics in unpolluted and polluted soils. *Environ. Toxicol. Chem.* 24, 499–509.
521 <https://doi.org/10.1897/04-231R.1>

522 Mia, S., Dijkstra, F.A., Singh, B., 2017. Long-Term Aging of Biochar : A Molecular Understanding With
523 Agricultural and Environmental Implications, 1st ed, *Advances in Agronomy*. Elsevier Inc.
524 <https://doi.org/10.1016/bs.agron.2016.10.001>

525 Moreno-Castilla, C., Ferro-Garcia, M.A., Joly, J.P., Bautista-Toledo, I., Carrasco-Marin, F., Rivera-Utrilla, J.,
526 1995. Activated carbon surface modifications by nitric acid, hydrogen peroxide, and ammonium
527 peroxydisulfate treatments. *Langmuir* 11, 4386–4392.

528 Mukherjee, A., Zimmerman, A.R., Hamdan, R., Cooper, W.T., 2014. Physicochemical changes in pyrogenic
529 organic matter (biochar) after 15 months of field aging 5194. <https://doi.org/10.5194/se-5-693-2014>

530 Nachenius, R.W., Ronsse, F., Venderbosch, R.H., Prins, W., 2013. Biomass Pyrolysis, in: Chemical Engineering
531 for Renewables Conversion. Elsevier Inc., pp. 75–139. [https://doi.org/10.1016/B978-0-12-386505-2.00002-](https://doi.org/10.1016/B978-0-12-386505-2.00002-X)
532 X

533 Oustriere, N., Marchand, L., Rosette, G., Friesl-Hanl, W., Mench, M., 2017. Wood-derived-biochar combined with
534 compost or iron grit for in situ stabilization of Cd, Pb, and Zn in a contaminated soil. *Environ. Sci. Pollut.*
535 *Res.* 24, 7468–7481. <https://doi.org/10.1007/s11356-017-8361-6>

536 Palansooriya, K.N., Shaheen, S., Chen, S.S., Tsang, D.C.W., Hashimoto, Y., Hou, D., Bolan, N.S., Rinklebe, J.,
537 Ok, Y.S., 2020. Soil amendments for immobilization of potentially toxic elements in contaminated soils : A
538 critical review. *Environ. Int.* 134, 105046. <https://doi.org/10.1016/j.envint.2019.105046>

539 Qi, F., Lamb, D., Naidu, R., Bolan, N.S., Yan, Y., Sik, Y., Mahmudur, M., Choppala, G., 2018. Cadmium solubility
540 and bioavailability in soils amended with acidic and neutral biochar. *Sci. Total Environ.* 611, 1457–1466.
541 <https://doi.org/10.1016/j.scitotenv.2017.08.228>

542 Qian, L., Chen, M., Chen, B., 2015. Competitive adsorption of cadmium and aluminum onto fresh and oxidized
543 biochars during aging processes. *J Soils Sediments* 1130–1138. <https://doi.org/10.1007/s11368-015-1073-y>

544 Rauret, G., López-Sánchez, J.F., Sahuquillo, A., Rubio, R., Davidson, C., Ure, A., Quevauviller, P., 1999.
545 Improvement of the BCR three step sequential extraction procedure prior to the certification of new sediment
546 and soil reference materials. *J. Environ. Monit.* 1, 57–61. <https://doi.org/10.1039/a807854h>

547 Rechberger, M. V, Kloss, S., Rennhofer, H., Tintner, J., Watzinger, A., Soja, G., Lichtenegger, H., Zehetner, F.,
548 2017. Changes in biochar physical and chemical properties : Accelerated biochar aging in an acidic soil.
549 *Carbon N. Y.* 115, 209–219. <https://doi.org/10.1016/j.carbon.2016.12.096>

550 Ronsse, F., Nachenius, R.W., Prins, W., 2015. Carbonization of Biomass, in: *Recent Advances in Thermo-*
551 *Chemical Conversion of Biomass.* pp. 293–324.

552 Ronsse, F., Van Hecke, S., Dickinson, D., Prins, W., 2013. Production and characterization of slow pyrolysis
553 biochar : influence of feedstock type and pyrolysis conditions. *Gcb Bioenergy* 5, 104–115.
554 <https://doi.org/10.1111/gcbb.12018>

555 Singh, B., Fang, Y., Cowie, B.C.C., Thomsen, L., 2014. Organic Geochemistry NEXAFS and XPS
556 characterisation of carbon functional groups of fresh and aged biochars 77, 1–10.

557 <https://doi.org/10.1016/j.orggeochem.2014.09.006>

558 Sun, J., Lian, F., Liu, Z., Zhu, L., Song, Z., 2014. Ecotoxicology and Environmental Safety Biochars derived from
559 various crop straws : Characterization and Cd (II) removal potential. *Ecotoxicol. Environ. Saf.* 106, 226–
560 231. <https://doi.org/10.1016/j.ecoenv.2014.04.042>

561 Tan, X., Liu, Y., Gu, Y., Zeng, G., Wang, X., Hu, X., Sun, Z., Yang, Z., 2015. Immobilization of Cd(II) in acid
562 soil amended with different biochars with a long term of incubation. *Environ. Sci. Pollut. Res.* 22, 12597–
563 12604. <https://doi.org/10.1007/s11356-015-4523-6>

564 Tessier, A., Campbell, P.G.C., Bisson, M., 1979. Sequential Extraction Procedure for the Speciation of Particulate
565 Trace Metals. *Anal. Chem.* 51, 844–851.

566 Van Poucke, R., Ainsworth, J., Maesele, M., Ok, Y.S., Meers, E., Tack, F.M.G., 2018. Chemical stabilization of
567 Cd-contaminated soil using biochar. *Appl. Geochemistry* 88, 122–130.
568 <https://doi.org/10.1016/j.apgeochem.2017.09.001>

569 Van Poucke, R., Meers, E., Tack, F.M.G., 2020. Leaching behavior of Cd, Zn and nutrients (K, P, S) from a
570 contaminated soil as affected by amendment with biochar. *Chemosphere* 245, 125561.
571 <https://doi.org/10.1016/j.chemosphere.2019.125561>

572 Van Ranst, E., Verloo, M., Demeyer, A., Pauwels, J., 1999. Manual for the soil chemistry and fertility laboratory:
573 analytical methods for soils and plants equipment, and management of consumables.

574 Wang, H.Y., Chen, P., Zhu, Y.G., Cen, K., Sun, G.X., 2019. Simultaneous adsorption and immobilization of As
575 and Cd by birnessite-loaded biochar in water and soil. *Environ. Sci. Pollut. Res.* 26, 8575–8584.
576 <https://doi.org/10.1007/s11356-019-04315-x>

577 Wang, L., Ok, Y.S., Tsang, D.C.W., Alessi, D.S., Rinklebe, J., Wang, H., Mašek, O., Hou, R., O'Connor, D., Hou,
578 D., 2020. New Trends in Biochar Pyrolysis and Modification Strategies: Feedstock, Pyrolysis Conditions,
579 Sustainability Concerns and Implications for Soil Amendment. *Soil Use Manag.* 1–29.
580 <https://doi.org/10.1111/sum.12592>

581 Weber, K., Quicker, P., 2018. Properties of biochar. *Fuel* 217, 240–261. <https://doi.org/10.1016/j.fuel.2017.12.054>

582 WHO, 2007. Health risks of heavy metals from long-range transboundary air pollution. World Health
583 Organization.

584 Xu, C., Chen, H. xiang, Xiang, Q., Zhu, H. hua, Wang, S., Zhu, Q. hong, Huang, D. you, Zhang, Y. zhu, 2018.
585 Effect of peanut shell and wheat straw biochar on the availability of Cd and Pb in a soil–rice (*Oryza sativa*
586 L.) system. *Environ. Sci. Pollut. Res.* 25, 1147–1156. <https://doi.org/10.1007/s11356-017-0495-z>

587 Xu, X., Cao, X., Zhao, L., Wang, H., Yu, H., Gao, B., 2013. Removal of Cu, Zn, and Cd from aqueous solutions
588 by the dairy manure-derived biochar. *Environ. Sci. Pollut. Res.* 20, 358–368.
589 <https://doi.org/10.1007/s11356-012-0873-5>

590 Xu, Y., Fang, Z., Tsang, E.P., 2016. In situ immobilization of cadmium in soil by stabilized biochar-supported
591 iron phosphate nanoparticles. *Environ. Sci. Pollut. Res.* 23, 19164–19172. [https://doi.org/10.1007/s11356-](https://doi.org/10.1007/s11356-016-7117-z)
592 [016-7117-z](https://doi.org/10.1007/s11356-016-7117-z)

593 Yang, X., Liu, J., McGrouther, K., Huang, H., Lu, K., Guo, X., He, L., Lin, X., Che, L., Ye, Z., Wang, H., 2016.
594 Effect of biochar on the extractability of heavy metals (Cd, Cu, Pb, and Zn) and enzyme activity in soil.
595 *Environ. Sci. Pollut. Res.* 23, 974–984. <https://doi.org/10.1007/s11356-015-4233-0>

596 Yang, Y., Heaven, S., Venetsaneas, N., Banks, C.J., Bridgwater, A. V, 2018. Slow pyrolysis of organic fraction of
597 municipal solid waste (OFMSW): Characterisation of products and screening of the aqueous liquid product
598 for anaerobic digestion. *Appl. Energy* 213, 158–168. <https://doi.org/10.1016/j.apenergy.2018.01.018>

599 Yu, Y., Yang, Y., Cheng, Z., Blanco, P.H., Liu, R., Bridgwater, A. V, Cai, J., 2016. Pyrolysis of Rice Husk and
600 Corn Stalk in Auger Reactor . 1 . Characterization of Char and Gas at Various Temperatures. *Energy &*
601 *Fuels*. <https://doi.org/10.1021/acs.energyfuels.6b02276>

602 Zhao, L., Cao, X., Mašek, O., Zimmerman, A., 2013. Heterogeneity of biochar properties as a function of feedstock
603 sources and production temperatures. *J. Hazard. Mater.* 256–257, 1–9.
604 <https://doi.org/10.1016/J.JHAZMAT.2013.04.015>

605 Zheng, R., Li, C., Sun, G., Xie, Z., Chen, J., Wu, J., Wang, Q., 2017. The influence of particle size and feedstock
606 of biochar on the accumulation of Cd, Zn, Pb, and As by *Brassica chinensis* L. *Environ. Sci. Pollut. Res.* 24,
607 22340–22352. <https://doi.org/10.1007/s11356-017-9854-z>

608 Zuo, X., Liu, Z., Chen, M., 2016. Bioresource Technology Effect of H₂O₂ concentrations on copper removal
609 using the modified hydrothermal biochar. *Bioresour. Technol.* 207, 262–267.
610 <https://doi.org/10.1016/j.biortech.2016.02.032>

ACCEPTED VERSION